2023 IEEE Wireless Communications and Networking Conference (WCNC) | 978-1-6654-9122-8/23/$31.00 ©2023 IEEE | DOI: 10.1109/WCNC55385.2023.10118918

RSMA Inspired User Cooperation in Hybrid VLC/RF Networks for Coverage Extension

Konstantinos G. Rallis*, Vasilis K. Papanikolaou*, Sotiris A. Tegos†, Alexis A. Dowhuszko‡, Panagiotis D. Diamantoulakis†, Mohammad-Ali Khalighi§, and George K. Karagiannidis*

*Department of Electrical and Computer Engineering, Aristotle University of Thessaloniki, GR-54124 Thessaloniki, Greece

†Department of Applied Informatics, University of Macedonia, 54636 Thessaloniki, Greece

‡Department of Communications and Networking, Aalto University, 02150 Espoo, Finland

§Aix-Marseille University, CNRS, Centrale Marseille, Institut Fresnel, Marseille, France

Emails: {konralgeo,vpapanikk,geokarag}@ece.auth.gr, sotiris.a.tegos@gmail.com, alexis.dowhuszko@aalto.fi, padiaman@ieee.org, ali.khalighi@fresnel.fr

***Abstract*—In this paper, we propose and evaluate a hybrid visible light communication (VLC)/radio-frequency (RF) network architecture, where a VLC access point serves two user equipments (UEs), which also act as RF relays in order to extend the network's coverage to a third UE outside the VLC cell. The proposed protocol is inspired by uplink rate-splitting multiple access to efficiently route the messages to the UEs. In more detail, the proposed protocol utilizes the nuances of the specific network architecture to efficiently utilize the wireless resource blocks for both coverage and throughput. The protocol is then optimized by maximizing the minimum achievable rate. Simulation results show that the proposed method achieves superior results compared with a more conventional benchmark scheme, that is also optimized under the same constraints.**

***Index Terms*—Visible light communications, resource allocation, max-min rate, hybrid VLC/RF, coverage extension**

I. Introduction

Visible light communication (VLC) networks are considered as a promising energy efficient alternative for enhanced indoor network access in future wireless access, as we pave the way for the sixth generation (6G). A blessing and a curse, the seemingly ultra small cells (e.g., atto-cells) that are created by the VLC access points (APs) allow for an ultra-dense VLC network to be built with a high frequency reuse factor. On top of that, VLC APs are built with highly energy efficient and low-cost light emitting diodes (LED) that are concurrently used for illumination purposes [1], [2]. However, to enable high data rates in VLC, usually a line-of-sight (LoS) component is required, so nodes being outside the coverage area of the VLC AP can severely impact performance. Furthermore, LoS can be blocked either by obstacles or by the device orientation. To counteract the aforementioned issues, the hybrid network topology with a radio-frequency (RF) sub-network has been promoted as an alternative. In this direction, hybrid VLC/RF networks have offered interesting results that showcase how the heterogeneous composite network offers the best of both worlds, i.e., high achievable rate, coverage, energy efficiency [3], [4].

Naturally, the combination of the hybrid VLC/RF network architecture is considered to operate with novel multiple access schemes to improve performance. Non-orthogonal multiple access (NOMA) techniques have been widely examined in this type of network with remarkable results [2], [5]. A less common, but very promising way to break orthogonality is rate-splitting multiple access (RSMA). Although RSMA enables the use of the available resources in a non-orthogonal way, it is based on a different principle compared to what is commonly referred as NOMA. Its main characteristic is its capability to provide important advantages compared to orthogonal multiple access (OMA) in terms of connectivity, delay, throughput, energy efficiency with acceptable complexity, which do not vanish under practical conditions. In brief, the key behind realizing these benefits is the ability of rate-splitting (RS) to partially decode interference and partially treat interference as noise by splitting messages. To this end, RSMA provides flexible decoding and, thus, a more general and robust transmission framework in comparison with the conventional NOMA mechanism.

In the existing literature, most works on RSMA investigate the downlink scenario. In downlink RSMA, the message transmitted to the users is divided into a common message and a private message. The common message is a message decoded by multiple users and the private message is a message that only a specific user intends to receive [6]. Therefore, adjusting the split of common and private messages can control the computational complexity and the data rate achieved by RSMA. To this direction, it was proven that downlink RSMA unifies NOMA and space-division multiple access for both RF [6] and VLC [7]. In the context of VLC, downlink RSMA was investigated in [8], where signal-to-interference and noise ratio expressions are derived and then used to evaluate the performance in terms of weighted sum rate in a two-user scenario. Moreover, in [9], one-layer RSMA was used in multi-cell indoor VLC networks by considering the Lambertian radiation model.

Regarding the uplink scenario, there is a subset of users that simultaneously transmit more messages than the number of users belonging in this subset. The utilized decoding order of the users' messages is not necessarily fixed, but it can be chosen by the AP, based on the instantaneous channel state information. It should be highlighted that uplink RSMA enables any point in the capacity region of the multiple access channel (MAC) to be achieved with successive decoding [10]. Specifically, in [11], the RS principle was applied in an uplink NOMA network and its performance in terms of outage probability and achievable sum rate was investigated. Moreover, in [12], an uplink NOMA network with RS consisting of two users was investigated and it was shown that the fairness among users and the outage performance improve. Also, in [13], the performance of an uplink RSMA network with two sources was investigated in terms of outage probability and throughput, considering all possible decoding orders. Furthermore, in [14], two novel cooperative-NOMA and cooperative-RSMA schemes were proposed for uplink user cooperation, the achievable rates were derived and two optimization problems were formulated to maximize the minimum rate of two users, while the performance in terms of ergodic rate was investigated in [15] for cognitive radio inspired NOMA and RSMA.

To this end, in the existing literature, the concept of RSMA has not been utilized in hybrid VLC-RF networks. Motivated by this, in this work, we investigate a hybrid VLC-RF network aiming to serve three user equipments (UEs). The two UEs, which are located inside the VLC AP coverage area, are served in an orthogonal way based on TDMA, ensuring interference free transmission and providing an additional degree of freedom as adaptive time allocation is utilized [16]. Considering that the third UE is located outside the coverage area of the VLC AP, the other two UEs act as half duplex relays and transmit through RF the third UE's message which has been encoded by the VLC AP in their respective messages. When the two UEs simultaneously transmit to the third UE, the principles of uplink RSMA are utilized. Focusing on the fairness of the proposed system, we maximize the minimum rate of the three UEs. The non-convex formulated optimization problem is transformed into a convex one and is solved. Simulations indicate the effectiveness of the proposed system compared to benchmarks.

II. System Model

We consider an indoor network, where a VLC AP, located L meters vertically from the receivers' plane, serves two UEs, namely U_1 and U_2. These UEs are located in the AP's coverage area, which is considered as a cyclic disk of radius D_{VLC}. A third UE, denoted as U_3, which is located outside the VLC coverage area, i.e., the annular area bounded by radii D_{VLC} and D_{RF} with $D_{\text{VLC}} > D_{\text{RF}}$, is served by half duplex relay RF links from the two VLC UEs. Utilizing polar coordinates, UEs' locations can be given by (ρ_i, θ_i) pairs.

A. VLC Transmission

The received signal at the i-th UE with $i \in \{1, 2\}$ is given by

$$y_i = \eta h_i^{\text{VLC}} x_i + n_i, \quad (1)$$

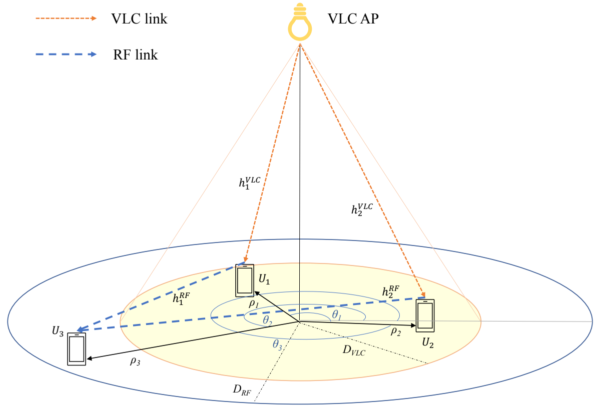

Fig. 1. System model

where η is the photodetector's responsivity, x_i is the transmitted signal to the i-th UE, and n_i is the additive white Gaussian noise at the i-th UE. The VLC channel gain is given by [1]

$$h_i^{\text{VLC}} = \frac{m+1}{2\pi d_i^2} A_r \cos^m(\phi_i) T_f g(\psi_i) \cos(\psi_i), \quad (2)$$

where A_r is the photodetector's area, ψ_i, ϕ_i are the incidence and irradiance angles, respectively, d_i denotes the distance between the VLC AP and UE i, and T_f is the optical filter gain. Assuming that the light source is Lambertian, m denotes the emission order, and is given by

$$m = -\frac{\ln 2}{\ln(\cos(\Phi_{1/2}))}, \quad (3)$$

where $\Phi_{1/2}$ is the transmitter's semi-angle at half power. The optical concentrator gain $g(\psi_i)$ is described as

$$g(\psi_i) = \begin{cases} \frac{n_c^2}{\sin^2 \Psi_{\text{FoV}}}, & 0 \le \psi_i \le \Psi_{\text{FoV}} \\ 0, & \psi_i > \Psi_{\text{FoV}}, \end{cases} \quad (4)$$

where Ψ_{FoV} is the field-of-view (FoV) of the receiver and n_c is the refractive index.

In order to approximate the achievable rate in VLC, we utilize the following lower bound [17]

$$\text{R}_i^{\text{VLC}} = B_{\text{VLC}} \log_2\left(1 + \frac{(\eta h_i^{\text{VLC}} P_{\text{VLC}})^2}{9\sigma^2(1+\epsilon_\mu)^2}\right) - \epsilon_\phi, \quad (5)$$

where σ^2 is the noise variance, P_{VLC} is the average constraint of the transmitted intensity, B_{VLC} is the VLC channel's bandwidth and $\epsilon_\mu = 0.0015$, $\epsilon_\phi = 0.016$.

B. RF Transmission

For the RF transmission, the Euclidean distance between the i-th UE and the RF UE is given by

$$d_{i,3}^{\text{RF}} = \sqrt{\rho_3^2 + \rho_i^2 - 2\rho_3\rho_i \cos(\theta_i - \theta_3)}, \; i = 1, 2. \quad (6)$$

The transmitted power P_{RF} is affected by path loss, which is modeled by the following formula $L_i^{\text{RF}} = (d_{i,3}^{\text{RF}}/d_0)^{-\zeta}$, where ζ denotes the path loss exponent, $d_0 = 1$ m is the reference distance. We consider Rayleigh fading, thus the RF channel coefficient $h_{\mathrm{RF}} \sim \mathcal{CN}(0,1)$. To this direction, the RF channel's capacity is directly given by Shannon's formula as

$$\mathrm{R}_i^{\mathrm{RF}} = B_{\mathrm{RF}} \log_2 \left(1 + \frac{L_i^{\mathrm{RF}} |h_i^{\mathrm{RF}}|^2 P_{\mathrm{RF}}}{\sigma_{\mathrm{RF}}^2}\right), \tag{7}$$

where σ_{RF}^2 is the noise variance and B_{RF} denotes the RF channel's bandwidth.

For the case that both VLC UEs transmitting to U_3, the concept of uplink RSMA is considered. In uplink RSMA, only one of the two UEs should split its message to achieve the entire capacity region [10], thus without loss of generality, we consider that the second UE splits its transmitted message into two parts, i.e., $x_2^{(\delta)}$ with $\delta \in \{1,2\}$ and allocates power $p_2^{(\delta)}$ to each of them. For these power levels is true $\sum_{\delta=1}^2 p_2^{(\delta)} \leq P_{\mathrm{RF}}^{\max}$ where $P_{\mathrm{RF}}^{\max}$ is the maximum power level available for transmission. Therefore, at the receiver's side, the signal can be written as

$$\begin{aligned} y_3^{\mathrm{RF}} = &\sqrt{L_1 p_1^{(2)}} h_1^{\mathrm{RF}} x_1 + \sqrt{L_2 p_2^{(2)}} h_2^{\mathrm{RF}} x_2^{(2)} \\ &+ \sqrt{L_2 p_2^{(1)}} h_2^{\mathrm{RF}} x_2^{(1)} + n_{\mathrm{RF}}, \end{aligned} \tag{8}$$

while the considered decoding order is $x_2^{(1)} \to x_1 \to x_2^{(2)}$ with the corresponding achievable rates being upper bounded, respectively, as

$$r_2^{(1)} \leq B_{\mathrm{RF}} \log_2 \left(1 + \frac{L_2 |h_2^{\mathrm{RF}}|^2 p_2^{(1)}}{L_1 |h_1^{\mathrm{RF}}|^2 p_1 + L_2 |h_2^{\mathrm{RF}}|^2 p_2^{(2)} + \sigma_{\mathrm{RF}}^2}\right), \tag{9}$$

$$r_1 \leq B_{\mathrm{RF}} \log_2 \left(1 + \frac{L_1 |h_1^{\mathrm{RF}}|^2 p_1}{L_2 |h_2^{\mathrm{RF}}|^2 p_2^{(2)} + \sigma_{\mathrm{RF}}^2}\right), \tag{10}$$

$$r_2^{(2)} \leq B_{\mathrm{RF}} \log_2 \left(1 + \frac{L_2 |h_2^{\mathrm{RF}}|^2 p_2^{(2)}}{\sigma_{\mathrm{RF}}^2}\right). \tag{11}$$

III. Proposed Protocol and Optimization Framework

We consider that before transmission, the VLC AP is updated with the requested messages x_i of all UEs. Next, the AP splits RF UE's message x_3 into three parts, i.e., $x_{1,3}^{(1)}$, $x_{1,3}^{(2)}$ and $x_{2,3}$ and then adds them to the VLC UEs' messages. To this end, the AP transmits $x_1 + x_{1,3}^{(1)} + x_{1,3}^{(2)}$ and $x_2 + x_{2,3}$ to U_1 and U_2, respectively, in a dynamic TDMA way. The downlink timeslot is split into three parts τ_k, where $k \in \mathcal{K} \triangleq \{1,2,3\}$ and it holds that

$$\tau_1 + \tau_2 + \tau_3 \leq 1, \quad 0 \leq \tau_k \leq 1. \tag{12}$$

- *During* τ_1: The first VLC UE receives and decodes with rate $\mathrm{R}_1^{\mathrm{VLC}}$ the message $x_1 + x_{1,3}^{(1)} + x_{1,3}^{(2)}$. Taking into account that these messages are independent and considering that the transmitting data rates should not exceed the VLC link's achievable rate, the following constraint arises

$$r_1 + r_{1,3}^{(1)} + r_{1,3}^{(2)} \leq \tau_1 R_1^{\mathrm{VLC}}. \tag{13}$$

- *During* τ_2: U_2 performs the same receiving process as U_1 did before. Thus, it holds

$$r_2 + r_{2,3} \leq \tau_2 R_2^{\mathrm{VLC}}. \tag{14}$$

Simultaneously, U_1 relays via RF link the message $x_{1,3}^{(1)}$. The achievable rate should not exceed the RF link's capacity, hence we require

$$r_{1,3}^{(1)} \leq \tau_2 R_1^{\mathrm{RF}}. \tag{15}$$

- *During* τ_3: Both VLC UEs are transmitting via RF link to the third UE utilizing RSMA. More specifically, U_2 splits $x_{2,3}$ into two parts, denoted by $x_{2,3}^{(1)}$ and $x_{2,3}^{(2)}$ and (14) can be rewritten as

$$r_2 + r_{2,3}^{(1)} + r_{2,3}^{(2)} \leq \tau_2 R_2^{\mathrm{VLC}}, \tag{16}$$

in order to ensure that U_2 received them during the previous timeslot. According to the considered RSMA scheme, (9), (10), and (11) are rewritten as

$$r_{2,3}^{(1)} \leq \tau_3 B_{\mathrm{RF}} \log_2 \left(1 + \frac{L_2 |h_2^{\mathrm{RF}}|^2 P_{2,3}^{(1)}}{L_2 |h_2^{\mathrm{RF}}|^2 P_{2,3}^{(2)} + L_1 |h_2^{\mathrm{RF}}|^2 P_{1,3}^{(2)} + \sigma_{\mathrm{RF}}^2}\right), \tag{17}$$

$$r_{1,3}^{(2)} \leq \tau_3 B_{\mathrm{RF}} \log_2 \left(1 + \frac{L_1 |h_1^{\mathrm{RF}}|^2 P_{1,3}^{(2)}}{L_2 |h_2^{\mathrm{RF}}|^2 P_{2,3}^{(2)} + \sigma_{\mathrm{RF}}^2}\right), \tag{18}$$

$$r_{2,3}^{(2)} \leq \tau_3 B_{\mathrm{RF}} \log_2 \left(1 + \frac{L_2 |h_2^{\mathrm{RF}}|^2 P_{2,3}^{(2)}}{\sigma_{\mathrm{RF}}^2}\right). \tag{19}$$

To this end, we formulate an optimization problem aiming to maximize the minimum rate of the considered system and we propose a low complexity solution for it.

$$\begin{aligned} \max_{\mathbf{r}, \mathbf{P}, \tau, R_{\min}} \quad & R_{\min} \\ \text{s.t.} \quad & \mathrm{C}_1 : r_1 + r_{1,3}^{(1)} + r_{1,3}^{(2)} \leq \tau_1 R_1^{\mathrm{VLC}}, \\ & \mathrm{C}_2 : r_2 + r_{2,3}^{(1)} + r_{2,3}^{(2)} \leq \tau_2 R_2^{\mathrm{VLC}}, \\ & \mathrm{C}_3 : r_{1,3}^{(1)} \leq \tau_2 R_1^{\mathrm{RF}}, \\ & \mathrm{C}_4 : (17),\ \mathrm{C}_5 : (18),\ \mathrm{C}_6 : (19), \\ & \mathrm{C}_7 : \tau_1 + \tau_2 + \tau_3 \leq 1, \\ & \mathrm{C}_8 : r_{1,3}^{(1)} + r_{1,3}^{(2)} + r_{2,3}^{(1)} + r_{2,3}^{(2)} \geq w_3 R_{\min}, \\ & \mathrm{C}_9 : r_i \geq w_i R_{\min},\ i \in \{1,2\}, \\ & \mathrm{C}_{10} : P_{\mathrm{VLC}} \leq P_{\mathrm{VLC}}^{\max}, \\ & \mathrm{C}_{11} : P_{2,3}^{(1)} + P_{2,3}^{(2)} \leq P_{\mathrm{RF}}^{\max}, \\ & \mathrm{C}_{12} : P_{1,3}^{(1)}, P_{1,3}^{(2)} \leq P_{\mathrm{RF}}^{\max}, \end{aligned} \tag{20}$$

where $\mathbf{r} = [r_i, \tilde{r}_{i,3}^{(\delta)}]$, $\mathbf{P} = [P_{\mathrm{VLC}}, P_{i,3}^{(\delta)}]$, $\tau = [\tau_k]$ and the weighting factors w_i are introduced to model the UEs' priority. This program is non-convex. The main issues are the expressions of $\mathrm{C}_1 - \mathrm{C}_6$, where τ_k are multiplied with logarithms. Squared term of VLC transmission power P_{VLC} and the uplink RSMA rate expressions also contribute to the non-convexity. We aim to transform (20) to an equivalent convex problem, in order to solve it in polynomial time. Thus, we apply the following transformations

$$R_{\min} = e^{\tilde{R}_{\min}}, \qquad r_i = e^{\tilde{r}_i}, \ \ i \in 1,2,$$
$$r_{i,3}^{(\delta)} = e^{\tilde{r}_{i,3}^{(\delta)}}, \qquad \tau_k = e^{\tilde{\tau}_k},$$
$$P_{\mathrm{VLC}} = \sqrt{p_{\mathrm{VLC}}}, \qquad P_{i,3}^{(\delta)} = e^{p_{i,3}^{(\delta)}}, \ \text{ if } P_{i,3}^{(\delta)} \neq P_{1,3}^{(1)}.$$

After some algebraic manipulations, problem (20) can be written as

$$\max_{\mathbf{r},\mathbf{P},\tau,\tilde{R}_{\min}} \ e^{\tilde{R}_{\min}} \tag{21}$$
$$\begin{aligned}
\textbf{s.t.} \quad & \mathrm{C}_1 : e^{\tilde{r}_1-\tilde{\tau}_1} + e^{\tilde{r}_{1,3}^{(1)}-\tilde{\tau}_1} + e^{\tilde{r}_{1,3}^{(2)}-\tilde{\tau}_1} \leq R_1^{\mathrm{VLC}} \\
& \mathrm{C}_2 : e^{\tilde{r}_2-\tilde{\tau}_2} + e^{\tilde{r}_{2,3}^{(1)}-\tilde{\tau}_2} + e^{\tilde{r}_{2,3}^{(2)}-\tilde{\tau}_2} \leq R_2^{\mathrm{VLC}} \\
& \mathrm{C}_3 : e^{\tilde{r}_{1,3}^{(1)}-\tilde{\tau}_2} \leq R_1^{\mathrm{RF}} \\
& \mathrm{C}_4 : \log(2^{e^{\tilde{r}_{2,3}^{(1)}-\tilde{\tau}_3}/B_{\mathrm{RF}}} - 1) - \log(L_1|h_1^{\mathrm{RF}}|^2) \\
& \quad + \log(L_2|h_2^{\mathrm{RF}}|^2 e^{p_{2,3}^{(2)}} + L_1|h_1^{\mathrm{RF}}|^2 e^{p_{1,3}^{(2)}} + \sigma_{\mathrm{RF}}^2) \\
& \quad - p_{2,3}^{(1)} \leq 0 \\
& \mathrm{C}_5 : \log(2^{e^{\tilde{r}_{1,3}^{(2)}-\tilde{\tau}_3}/B_{\mathrm{RF}}} - 1) - \log(L_2|h_2^{\mathrm{RF}}|^2) \\
& \quad + \log(L_2|h_2^{\mathrm{RF}}|^2 e^{p_{2,3}^{(2)}} + \sigma_{\mathrm{RF}}^2) - p_{1,3}^{(2)} \leq 0 \\
& \mathrm{C}_6 : \log(2^{e^{\tilde{r}_{2,3}^{(2)}-\tilde{\tau}_3}/B_{\mathrm{RF}}} - 1) - \log(L_2|h_2^{\mathrm{RF}}|^2) \\
& \quad - p_{2,3}^{(2)} + \log(\sigma_{\mathrm{RF}}^2) \leq 0 \\
& \mathrm{C}_7 : e^{\tau_1} + e^{\tau_2} + e^{\tau_3} \leq 1 \\
& \mathrm{C}_8 : e^{\tilde{r}_{1,3}^{(1)}} + e^{\tilde{r}_{1,3}^{(2)}} + e^{\tilde{r}_{2,3}^{(1)}} + e^{\tilde{r}_{2,3}^{(2)}} \geq w_3 e^{\tilde{R}_{\min}} \\
& \mathrm{C}_9 : \tilde{R}_{\min} + \log(w_i) - \tilde{r}_i \leq 0, \ i \in \{1,2\} \\
& \mathrm{C}_{10} : p_{\mathrm{VLC}} \leq (P_{\mathrm{VLC}}^{\max})^2 \\
& \mathrm{C}_{11} : e^{p_{2,3}^{(1)}} + e^{p_{2,3}^{(2)}} \leq P_{\mathrm{RF}}^{\max} \\
& \mathrm{C}_{12} : P_{1,3}^{(1)}, e^{p_{1,3}^{(2)}} \leq P_{\mathrm{RF}}^{\max}.
\end{aligned}$$

Here, C_1, C_2 and C_3 are convex, since their left-hand sides are sum of exponential functions and their right sides are concave as logarithmic functions. The Hessian matrix of the first term of C_4 is given by

$$\mathbf{H} = \begin{bmatrix} \frac{\partial^2 g}{\partial \tilde{r}_{2,3}^{(1)2}} & \frac{\partial^2 g}{\partial \tilde{r}_{2,3}^{(1)} \partial \tilde{\tau}_3} \\ \frac{\partial^2 g}{\partial \tilde{\tau}_3 \partial \tilde{r}_{2,3}^{(1)}} & \frac{\partial^2 g}{\partial \tilde{\tau}_3^2} \end{bmatrix} = \begin{bmatrix} q & -q \\ -q & q \end{bmatrix}. \tag{22}$$

It can be shown that the eigenvalues of matrix $\mathbf{H}$ are

$$\begin{aligned} \upsilon_1 &= 2q = \frac{2^g g \log(2)(2^g - g\log(2) - 1)}{(2^g-1)^2} \\ \upsilon_2 &= 0, \end{aligned} \tag{23}$$

where $g = e^{\tilde{r}_{2,3}^{(1)}-\tilde{\tau}_3}/B_{\mathrm{RF}}$.

Taking into account that $\psi = 2^g - g\log(2) - 1$ is an increasing function of g, and when $\tilde{r}_{2,3}^{(1)} - \tilde{\tau}_3 \to -\infty$, $g \to 0$ and $\psi \to 0$, it can easily be proven that $\upsilon_1 > 0$. This leads to the conclusion that the first term of C_4 is convex and considering that the rest terms are a log-sum-exp term and an affine one, C_4 is proven to be convex. With the same procedure, it is also shown that C_5 and C_6 are convex. C_7 and C_{11} are convex as sum of exponential terms and the rest constraints, i.e., C_9, C_{10}, C_{12}, are convex as they contain only exponential and affine terms. The objective function has now been transformed into a convex one, but since (21) is a maximization problem, it needs to be concave. Thus, we consider maximizing $\tilde{R}_{\min}$, which is equivalent to maximizing $e^{\tilde{R}_{\min}}$, since its an increasing one-by-one function of $\tilde{R}_{\min}$. Also, C_8 is still non-convex, but it can be written as difference of convex function as follows

$$\mathrm{C}_8 : w_i e^{\tilde{R}_{\min}} - e^{\tilde{r}_{1,3}^{(1)}} - e^{\tilde{r}_{1,3}^{(2)}} - e^{\tilde{r}_{2,3}^{(1)}} - e^{\tilde{r}_{2,3}^{(2)}} \leq 0. \tag{24}$$

Following that, we can solve the optimization problem in a tractable way, utilizing the successive convex approximation (SCA) iterative algorithm. We first approximate C_8's concave part, i.e., $f_c = e^{\tilde{r}_{1,3}^{(1)}} + e^{\tilde{r}_{1,3}^{(2)}} + e^{\tilde{r}_{2,3}^{(1)}} + e^{\tilde{r}_{2,3}^{(2)}}$, with its first order Taylor expansion as

$$\begin{aligned} T_{f_c}^j = f_c^j &+ \frac{\partial f_c^j}{\partial \tilde{r}_{1,3}^{(1)}}(\tilde{r}_{1,3}^{(1)} - \tilde{r}_{1,3}^{(1),j}) + \frac{\partial f_c^j}{\partial \tilde{r}_{1,3}^{(2)}}(\tilde{r}_{1,3}^{(2),j} - \tilde{r}_{2,3}^{(2),j}) \\ &+ \frac{\partial f_c^j}{\partial \tilde{r}_{2,3}^{(1)}}(\tilde{r}_{2,3}^{(1)} - \tilde{r}_{2,3}^{(1),j}) + \frac{\partial f_c^j}{\partial \tilde{r}_{2,3}^{(2)}}(\tilde{r}_{2,3}^{(2),j} - \tilde{r}_{2,3}^{(2),j}), \end{aligned} \tag{25}$$

where j is the iteration index of SCA algorithm and f_c^j, $\frac{\partial f_c^j}{\partial r_{i,3}^{(\delta)}}$ are the evaluations of f_c and $\frac{\partial f_c}{\partial \tilde{r}_{i,3}^{(\delta)}}$, respectively, at $\tilde{r}_{i,3}^{(\delta),j}$. This approximation enables the conversion of the non-convex part of C_8 into an affine one making it convex. After the equivalent change in the objective function and the linearization of C_8, the optimization problem can be re-written as

$$\max_{\mathbf{r},\mathbf{P},\tau,\tilde{R}_{\min}} \ \tilde{R}_{\min} \tag{26}$$
$$\begin{aligned}
\textbf{s.t.} \quad & \mathrm{C}_1 : e^{\tilde{r}_1-\tilde{\tau}_1} + e^{\tilde{r}_{1,3}^{(1)}-\tilde{\tau}_1} + e^{\tilde{r}_{1,3}^{(2)}-\tilde{\tau}_1} \leq R_1^{\mathrm{VLC}} \\
& \mathrm{C}_2 : e^{\tilde{r}_2-\tilde{\tau}_2} + e^{\tilde{r}_{2,3}^{(1)}-\tilde{\tau}_2} + e^{\tilde{r}_{2,3}^{(2)}-\tilde{\tau}_2} \leq R_2^{\mathrm{VLC}} \\
& \mathrm{C}_3 : e^{\tilde{r}_{1,3}^{(1)}-\tilde{\tau}_2} \leq R_1^{\mathrm{RF}} \\
& \mathrm{C}_4 : \log(2^{e^{\tilde{r}_{2,3}^{(1)}-\tilde{\tau}_3}/B_{\mathrm{RF}}} - 1) - \log(L_1|h_1^{\mathrm{RF}}|^2) \\
& \quad + \log(L_2|h_2^{\mathrm{RF}}|^2 e^{p_{2,3}^{(2)}} + L_1|h_1^{\mathrm{RF}}|^2 e^{p_{1,3}^{(2)}} + \sigma_{\mathrm{RF}}^2) \\
& \quad - p_{2,3}^{(1)} \leq 0 \\
& \mathrm{C}_5 : \log(2^{e^{\tilde{r}_{1,3}^{(2)}-\tilde{\tau}_3}/B_{\mathrm{RF}}} - 1) - \log(L_2|h_2^{\mathrm{RF}}|^2) \\
& \quad + \log(L_2|h_2^{\mathrm{RF}}|^2 e^{p_{2,3}^{(2)}} + \sigma_{\mathrm{RF}}^2) - p_{1,3}^{(2)} \leq 0 \\
& \mathrm{C}_6 : \log(2^{e^{\tilde{r}_{2,3}^{(2)}-\tilde{\tau}_3}/B_{\mathrm{RF}}} - 1) - \log(L_2|h_2^{\mathrm{RF}}|^2) \\
& \quad - p_{2,3}^{(2)} + \log(\sigma_{\mathrm{RF}}^2) \leq 0 \\
& \mathrm{C}_7 : e^{\tau_1} + e^{\tau_2} + e^{\tau_3} \leq 1 \\
& \mathrm{C}_8 : w_3 e^{\tilde{R}_{\min}} - T_{f_c}^k \leq 0 \\
& \mathrm{C}_9 : \tilde{R}_{\min} + \log(w_i) - \tilde{r}_i \leq 0 \\
& \mathrm{C}_{10} : p_{\mathrm{VLC}} \leq (P_{\mathrm{VLC}}^{\max})^2 \\
& \mathrm{C}_{11} : e^{p_{2,3}^{(1)}} + e^{p_{2,3}^{(2)}} \leq P_{\mathrm{RF}}^{\max} \\
& \mathrm{C}_{12} : P_{1,3}^{(1)}, e^{p_{1,3}^{(2)}} \leq P_{\mathrm{RF}}^{\max},
\end{aligned}$$

Algorithm 1: SCA Algorithm

Initialization: Set the initial point z_0. Also set iteration index $j = 0$ and the convergence accuracy ϵ;

while $C_{\text{SCA}} > \epsilon$ *(for given ϵ)* **do**

  Calculate an optimal solution z_{j+1} of problem (26);

  Let $C_{\text{SCA}} = ||z_j - z_{j+1}||_2$;

  $j \leftarrow j + 1$;

end

Result: optimal z^+_{j+1}

which is a convex one and it can be solved by standard convex procedures. We define $z = [\mathbf{r}, \mathbf{P}, \tau]$ as the set of the optimization variables. According to SCA iterative procedure, we first set an initial point defined as z_0 for $j = 0$. Next, we solve (26) utilizing conventional convex optimization algorithms (such as interior-point) iteratively and we obtain the solutions z_{j+1}. In each iteration, we update the index $j = j+1$ and we calculate the convergence value $C_{\text{SCA}} = ||z_j - z_{j+1}||_2$. We break when we reach the convergence criterion defined as $C_{\text{SCA}} \leq \epsilon$, where ϵ denotes the desired accuracy. This procedure is presented in Algorithm 1.

IV. Simulation Results and Discussion

In this section, numerical results from Monte Carlo simulations are presented and discussed. The results are obtained with the use of 10^4 realizations of UEs' random locations. SCA algorithm's accuracy ϵ is set equal to 10^{-6}. Unless otherwise stated, the parameters of the simulation are presented at Table I. It is noted that the radii of the coverage areas are considered as $D_{\text{VLC}} = L \times \tan(\Psi_{\text{FoV}})$ and $D_{\text{RF}} = D_{\text{VLC}} + 1.5$ measured in meters. Additionally, bandwidths of VLC and RF subsystem are normalized fulfilling the equality $B_{\text{VLC}} = 4B_{\text{RF}}$.

TABLE I
Simulation Parameters

Parameter	Value	Parameter	Value
$P^{\text{RF}}_{\text{max}}$	200 mW	σ^2	10^{-16}
A_r	1 cm^2	σ^2_{RF}	$10^{-13}B_{\text{RF}}$
L	1.5 m	T_f	1
ζ	2	Ψ_{FoV}	$\pi/3$
n_c	1.5	$\Phi_{1/2}$	$\pi/3$
η	0.53 A/W		

In order to compare the proposed protocol with a more conventional scenario, a benchmark scheme, where no RF transmission takes place during τ_2, is considered. According to this benchmark, U_3 receives the entirety of its message via uplink RSMA during τ_3. Benchmark scheme is optimized following the same steps as in the previous section. In addition, two network QoS configuration cases are investigated. Case 1 denotes the scenario where all UEs have the same requirements (i.e., $w_i = 1/3$), while case 2 stands for prioritizing the QoS of U_3. For case 2, the weight settings are $w_1 = w_2 = 1/6$ and $w_3 = 2/3$.

The superiority of the proposed protocol over the considered benchmark is clearly presented in Fig. 2 for both cases. In more detail, in this figure, the optimal $R_{\min}$ with respect to $P^{\max}_{\text{VLC}}$ is investigated. UEs are able to achieve better spectral efficiency in an equal weight configuration (i.e., case 1). More specifically, the proposed protocol offers around 36% improvement in minimum spectral efficiency for 1 W of transmit power over the benchmark scheme. For case 2, where U_3's performance is prioritized, a similar trend is observed. The proposed protocol outperforms the benchmark significantly. To be more precise, the proposed protocol requires less than a fifth of the transmitted power to achieve a minimum spectral efficiency of almost 29 bps/Hz. For transmit power of 1 W, the proposed protocol offers around 30% better spectral efficiency than the benchmark.

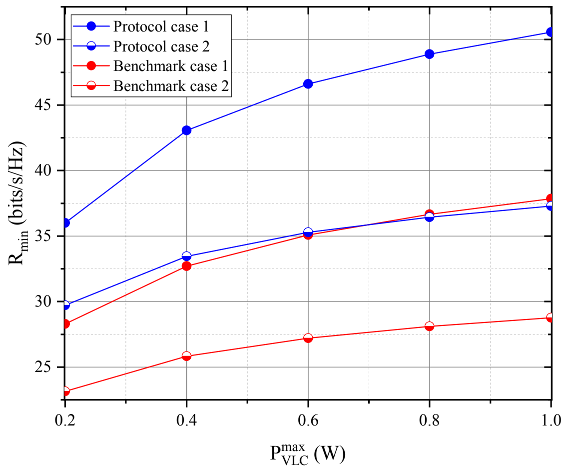

Fig. 2. $R_{\min}$ vs $P^{\max}_{\text{VLC}}$ for case 1 ($w_i = 1/3$) and case 2 ($w_1 = w_2 = 1/6$, $w_3 = 2/3$).

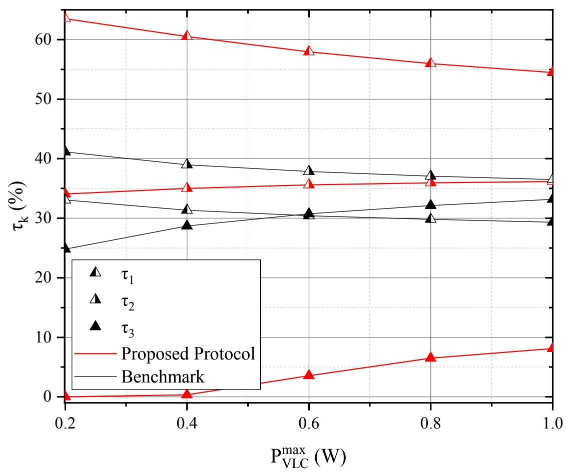

Fig. 3. Comparison of the optimal time portions for case 1 ($w_i = 1/3$)

In Fig 3, the optimal time allocation is illustrated with respect to $P^{\max}_{\text{VLC}}$ in case 1. Interestingly, over 90% of time is allocated to the first two timeslots. while for the benchmark all timeslots have similar duration. For this setup, the optimality is nearly achieved when the RF UE is served by one VLC UE at a time, not simultaneously. This fact is an advantage of the

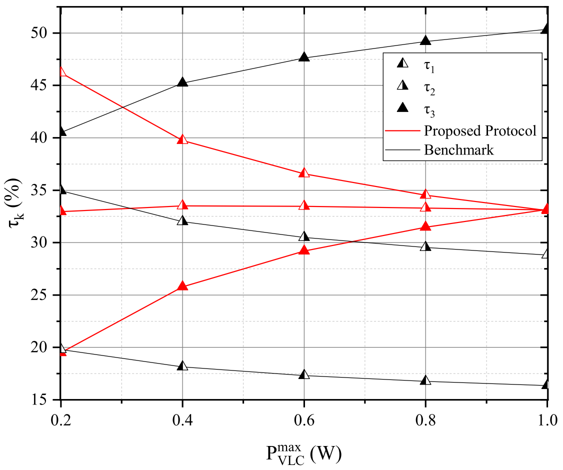

Fig. 4. Comparison of the optimal time portions for case 2 ($w_1 = w_2 = 1/3$, $w_3 = 2/3$)

non-interfering coexistence of the two technologies.

Finally, the time allocation of the proposed protocol is illustrated in Fig 4, prioritizing U_3, according to case 2. The duration of RF transmission via only one VLC UE is steady, while the simultaneous transmission utilizing RSMA increases while more power is consumed by the VLC AP. It is worth noting that, in the benchmark scheme, since it is not allowed a user to access the RF channel exclusively, the system is forced to allocate bigger portion of time to the RSMA broadcast.

V. Conclusion

In this paper, the possibility to extend the coverage of a VLC network has been examined through the use of cooperative RF relaying between UEs. In more detail, a pair of VLC UEs can utilize an RSMA inspired scheme to forward via RF links a message intended for a third UE, which is located outside the VLC cell coverage. The proposed protocol has been optimized aiming to maximize the weighted minimum achievable rate in the system, i.e., to fulfill the QoS constraints of the UEs and simulation results have been obtained to evaluate its performance. Ultimately, the superiority of the proposed protocol has been proven by comparing it to a benchmark scheme for a variety of system parameters.

Acknowledgement

This publication has been based upon work from COST Action CA19111 NEWFOCUS, supported by COST (European Cooperation in Science and Technology). The work of V. K. Papanikolaou was co-financed by Greece and the European Union (European Social Fund-ESF) through the Operational Programme "Human Resources Development, Education and Lifelong Learning" in the context of the Act "Enhancing Human Resources Research Potential by undertaking a Doctoral Research" Sub-action 2: IKY Scholarship Programme for PhD candidates in the Greek Universities. The work of S. A. Tegos and P. D. Diamantoulakis was supported by the Hellenic Foundation for Research and Innovation (H.F.R.I.) under the "3rd Call for H.F.R.I. Research Projects to support Post- Doctoral Researchers" (Project Number: 7280). The work of G. K. Karagiannidis was supported by the European Union's Horizon 2020 Research and Innovation Program under Agreement 957406.

References

[1] V. K. Papanikolaou, P. D. Diamantoulakis, and G. K. Karagiannidis, *Hybrid Lightwave/RF Connectivity for 6G Wireless Networks*. Cham: Springer International Publishing, 2021, pp. 169–186. [Online]. Available: https://doi.org/10.1007/978-3-030-72777-2_9

[2] K. G. Rallis, V. K. Papanikolaou, P. D. Diamantoulakis, A. A. Dowhuszko, J. Hämäläinen, and G. K. Karagiannidis, "Design of MAC-layer Protocols for Distributed NOMA-based VLC Networks," in *Proc. 13th Int. Symp. Commun. Syst., Netw., Digital Signal Process. (CSNDSP)*, Porto, Portugal, 2022, pp. 32–37.

[3] V. K. Papanikolaou, P. D. Diamantoulakis, P. C. Sofotasios, S. Muhaidat, and G. K. Karagiannidis, "On Optimal Resource Allocation for Hybrid VLC/RF Networks With Common Backhaul," *IEEE Trans. Cogn. Commun. Netw.*, vol. 6, no. 1, pp. 352–365, 2020.

[4] K. G. Rallis, V. K. Papanikolaou, P. D. Diamantoulakis, M.-A. Khalighi, and G. K. Karagiannidis, "Energy Efficiency Maximization in Cooperative Hybrid VLC/RF Networks with NOMA," in *Proc. 17th Int. Symp. Wireless Commun. Syst. (ISWCS)*, Berlin, Germany, 2021, pp. 1–6.

[5] V. K. Papanikolaou, P. D. Diamantoulakis, and G. K. Karagiannidis, "User Grouping for Hybrid VLC/RF Networks With NOMA: A Coalitional Game Approach," *IEEE Access*, vol. 7, pp. 103 299–103 309, Jul. 2019.

[6] B. Clerckx, Y. Mao, R. Schober, and H. V. Poor, "Rate-Splitting Unifying SDMA, OMA, NOMA, and Multicasting in MISO Broadcast Channel: A Simple Two-User Rate Analysis," *IEEE Wireless Commun. Lett.*, vol. 9, no. 3, pp. 349–353, Mar. 2020.

[7] S. Naser, P. C. Sofotasios, L. Bariah, W. Jaafar, S. Muhaidat, M. Al-Qutayri, and O. A. Dobre, "Rate-Splitting Multiple Access: Unifying NOMA and SDMA in MISO VLC Channels," *IEEE Open J. Vehic. Technol.*, vol. 1, pp. 393–413, Oct. 2020.

[8] S. Naser, L. Bariah, W. Jaafar, S. Muhaidat, P. C. Sofotasios, M. Al-Qutayri, and O. A. Dobre, "Optical Rate-Splitting Multiple Access for Visible Light Communications," 2020. [Online]. Available: https://arxiv.org/abs/2002.07583

[9] S. Tao, H. Yu, Q. Li, Y. Tang, and D. Zhang, "One-Layer Rate-Splitting Multiple Access with Benefits over Power-Domain NOMA in Indoor Multi-Cell Visible Light Communication Networks," in *IEEE Int. Conf. Commun. Workshops (ICC Workshops)*, Dublin, Ireland, 2020, pp. 1–7.

[10] B. Rimoldi and R. Urbanke, "A Rate-Splitting Approach to the Gaussian Multiple-Access Channel," *IEEE Trans. Inf. Theory*, vol. 42, no. 2, pp. 364–375, Mar. 1996.

[11] Y. Zhu, X. Wang, Z. Zhang, X. Chen, and Y. Chen, "A Rate-Splitting Non-Orthogonal Multiple Access Scheme for Uplink Transmission," in *Proc. 9th Int. Conf. Wireless Commun. and Signal Process. (WCSP)*, Nanjing, China, 2017, pp. 1–6.

[12] H. Liu, T. A. Tsiftsis, K. J. Kim, K. S. Kwak, and H. V. Poor, "Rate Splitting for Uplink NOMA with Enhanced Fairness and Outage Performance," *IEEE Trans. Wireless Commun.*, vol. 19, no. 7, pp. 4657–4670, Jul. 2020.

[13] S. A. Tegos, P. D. Diamantoulakis, and G. K. Karagiannidis, "On the Performance of Uplink Rate-Splitting Multiple Access," *IEEE Commun. Lett.*, vol. 26, no. 3, pp. 523–527, Mar. 2022.

[14] O. Abbasi and H. Yanikomeroglu, "Transmission Scheme, Detection and Power Allocation for Uplink User Cooperation with NOMA and RSMA," 2022. [Online]. Available: https://arxiv.org/abs/2201.04572

[15] Y. Xiao, S. A. Tegos, P. D. Diamantoulakis, Z. Ma, and G. K. Karagiannidis, "On the Ergodic Rate of Cognitive Radio Inspired Uplink Multiple Access," *IEEE Commun. Lett.*, vol. 27, no. 1, pp. 95–99, Jan. 2023.

[16] A. M. Abdelhady, O. Amin, A. Chaaban, B. Shihada, and M.-S. Alouini, "Downlink Resource Allocation for Dynamic TDMA-Based VLC Systems," *IEEE Trans. Wireless Commun.*, vol. 18, no. 1, pp. 108–120, Oct. 2019.

[17] A. Chaaban, Z. Rezki, and M.-S. Alouini, "On the Capacity of the Intensity-Modulation Direct-Detection Optical Broadcast Channel," *IEEE Trans. Wireless Commun.*, vol. 15, no. 5, pp. 3114–3130, Jan. 2016.